COBEM UBERLÂNDIA 2019

ABCM Associação Brasileira de Engenharia e Ciências Mecânicas

25th ABCM International Congress of Mechanical Engineering
October 20-25, 2019, Uberlândia, MG, Brazil

ANALYSIS OF PHONONIC CRYSTALS WITH UNCERTAINTY PARAMETERS

Marcela Rodrigues Machado
University of Brasília
marcelam@unb.br
Edson Jansen Pedrosa Miranda Junior
Federal Institute of Maranhão
edson.jansen@ifma.edu.br
José Maria Campos dos Santos
University of Campinas
zema@fem.unicamp.br

Abstract. *In this paper, the plane wave expansion (PWE) method is used to obtain the band structure of 1D phononic crystals (PnCs). Inherent to all real systems, geometry, material property and boundary condition uncertainties can be included in the model to evaluate the system uncertainty. The main goal is to analyse the effect of uncertainties in parameters of the metamaterials-based structures and how it can influence the Bragg-type band gaps of 1D PnC rods. The band structure is obtained and presented by including the effect of the uncertainty in the Young's modulus.*

Keywords: *Plane wave expansion , Band gap, Phononic crystal, Uncertainty quantification*

1. INTRODUCTION

The plane wave expansion - PWE is the most used method to calculate the band structure of periodic systems, such as photonic crystals (El-Naggar, 2012), PnCs (Kushwaha *et al.*, 1994; Sigalas and Economou, 1992; Laude *et al.*, 2009), sonic crystals (Kushwaha *et al.*, 1994) and mechanical metamaterials (Xiao *et al.*, 2012b,a). The PWE has also been applied to calculate the band structure of smart PnCs, by using the piezoelectric (Qian *et al.*, 2008), piezomagnetic (Vasseur *et al.*, 2011), and magnetoelectroelastic (Wang *et al.*, 2008) PnCs. The PWE uses the system periodicity and Floquet-Bloch's theorem to solve the wave equation, obtaining an eigenvalue problem $\omega(k)$. This eigenvalue problem must be solved for each Bloch wave vector value into the first irreducible Brillouin zone (FIBZ). One of the main advantages of using the PWE method is its facility for being implemented. PWE is regarded as a semi-analytical method because Fourier series expansion in reciprocal space must be truncated. This method has also some drawbacks, for instance, when there is high geometry or material mismatch PWE presents slow convergence.

Quantifying uncertainty in numerically simulated results is not recent. However, during the last few years, this research area has undergone remarkable development, in special for dynamic systems. The method commonly used is Monte Carlo (MC) simulation (Sobol', 1994). The MC simulation is a sampling method that consists in generates independent realizations of random variables based on their probability distributions. By solving the deterministic problem for each realization, and collecting an ensemble of solutions statistical moments can be calculated (Sobol', 1994). A large number of samples are needed to obtain the convergence, which means high computational cost in some cases. Otherwise, non sampling approaches such as the Perturbation Method may be used. It consists in expanding random fields in a truncated Taylor series around their mean (Xiu, 2010). The Direct Method consists in applying the moment equations to obtain the random solutions. The unknowns are the moments and their equations are derived by taking averages over the original stochastic governing equations.

The main goal of this paper is to use the PWE to formulate the 1D PnC rods and include uncertainty in the Young's modulus. The implemented technique is validated by comparing the deterministic and with the first and second statistical moments of the band structure. The MC simulation is adopted to generate the samples used to evaluated the statistical analysis.

2. MONTE CARLO SIMULATION

The Monte Carlo simulation has been used for decades. It is a method based on random samples used in approximations. The name itself is taken from the famous casino located in MC (Sampaio and Lima, 2012). The principle of the MC method is to simulate a large number of samples then compute for each sample the response quantity under consideration and then perform a statistical treatment of the sample population. Simulation methods are also named exact

methods, because the simulation result leads to exact outcomes when the sample number goes to infinity. To avoid certain approximations which occur in analytical methods and to be a non-intrusive method are another advantages of this type of techniques. Thus, the general idea of the method is solving mathematical problems by the simulation of random variables (Sobol', 1994). The MC method example of application is the multidimensional integral approximation. Supposing the integral of a given real multidimensional function g in a certain region $B \subset \mathbb{R}$,

$$I = \int_B g(\theta) d(\theta) \tag{1}$$

If g is a simple function, its integral (I) can be calculated easily. However, if g is a difficult function or is defined in a region with complicated contour can does not exist a closed form for (I). In such cases, numerical integration methods must be applied for if approximations for (I), such as the trapeze method, Simpson method and MC simulation. Assuming that (I) is one-dimensional integral, p is the function probability density of a random variable θ, rewriting equation (1) it is

$$I = \int_B h(\theta) p(\theta) d(\theta) \tag{2}$$

where $h(\theta) = g(\theta)/p(\mathbf{x}) \forall \theta \in B$. The integral I can be interpreted as the expected value of $h(\theta)$, it is:

$$I = \mathbb{E}[h(\theta)] = \int_B h(\theta) p(\theta) d(\theta) \tag{3}$$

Thus, and approximation $(\hat{I})$ for the integral can be expressed as

$$\hat{I} = \sum_{i=1}^{n} h(\theta^i) \tag{4}$$

where $\theta(1), \theta(2), ..., \theta(n)$ are samples of the random vector $\mathbf{\Theta}$ with probability density function p.

The mean and the standard deviation of the result are calculated through the samples generated. Let $X(\xi, \omega)$ be the frequency response of the stochastic system calculated for a realization ξ, generated by the MC method (Rubinstein, 2008). The mean-square convergence analysis with respect to independent realizations of the random variable θ, denoted by $\Theta_j(\xi, \omega)$, is carried out studying the function $n_S \mapsto conv(n_S)$ defined by:

$$conv(n_S) = \frac{1}{n_S} \sum_{j=1}^{n_S} \int_B \left\| \Theta_j(\xi, \omega) \right\|^2 d\omega \tag{5}$$

3. PWE FORMULATION FOR 1D PHONONIC CRYSTAL ROD WITH UNCERTAINTY PARAMETER

From the simple rod theory with the uncertainty parameter included in the model na represented by the variable $theta$, the governing equation for longitudinal vibrations in a 1D PnC can be written as:

$$\frac{\partial}{\partial x}\left[E(x,\theta) A \frac{\partial u(x,t)}{\partial x}\right] = \rho(x) A \frac{\partial^2 u(x,t)}{\partial t^2}, \tag{6}$$

where $u(x,t)$ is the axial displacement, x is the spatial position, t is time, $E(x,\theta)$ is the Young's modulus with random properties, A is the cross section area and $\rho(x)$ is the mass density. It is assumed that the 1D phononic crystal rod has a periodic material variation given by $E(x,\theta) = E(x+a,\theta)$ and $\rho(x) = \rho(x+a)$, where a is the lattice parameter, *i.e.*, the unit cell length.

Applying the temporal Fourier transform on Eq. 6, one obtains (Doyle, 1997):

$$\frac{\partial}{\partial x}\left[E(x,\theta) A \frac{\partial \hat{u}(x,\omega)}{\partial x}\right] + \omega^2 \rho(x) A \hat{u}(x,\omega) = 0, \tag{7}$$

where $\hat{u}(x,\theta,\omega)$ is the axial displacement on frequency domain and ω is the angular frequency. As the Young's modulus is a random variable, it is a linear system that will make the axial displacement random as well. Thus, by applying the Floquet-Bloch periodic boundary condition of the solution in x and considering one-dimensional wave propagation, one obtains

$$\hat{u}(x,\theta,\omega) = \tilde{u}(x,\theta) e^{jk(\omega)x}, \tag{8}$$

with the Bloch wave amplitude $\tilde{u}(x,\theta)$ periodic of period a, *i.e.*, $\tilde{u}(x,\theta) = \tilde{u}(x+a,\theta)$. k is the Bloch wave vector (here being scalar), also known as wave number. The wave vector has its value within the first irreducible Brillouin zone (FIBZ), in the reciprocal space, $[0, \pi/a]$, or within the first Brillouin zone (FBZ), $[-\pi/a, \pi/a]$.

Expanding the Bloch wave amplitude $\tilde{u}(x,\theta)$ as a Fourier series in the reciprocal space, omitting the frequency dependence of k, yields

$$\hat{u}(x,\theta,\omega) = \left(\sum_{m=-\infty}^{+\infty} \tilde{u}_m e^{jg_m x}\right) e^{jkx} = \sum_{m=-\infty}^{+\infty} \tilde{u}_m e^{j(k+g_m)x}, \tag{9}$$

where $\tilde{u}_m$ are the coefficients of the Fourier series of $\tilde{u}(x,\theta)$ and $g_m = 2\pi m/a$ is the reciprocal lattice vector. Note that g is a constant, since a one-dimensional periodicity is considered. Furthermore, the Young's modulus and the mass density can also be expanded as Fourier series in the reciprocal space as

$$E(x,\theta) = \sum_{n=-\infty}^{+\infty} E_n e^{jg_n x},\ \rho(x) = \sum_{n=-\infty}^{+\infty} \rho_n e^{jg_n x}, \tag{10}$$

where $g_n = 2\pi n/a$. Note that the Fourier series coefficients E_n and ρ_n in Eq. 10 can be computed using

$$E_n = \frac{1}{a}\int_{-a/2}^{a/2} E(x,\theta) e^{-jg_n x} dx,\ \rho_n = \frac{1}{a}\int_{-a/2}^{a/2} \rho(x) e^{-jg_n x} dx. \tag{11}$$

Substituting Eqs. 9 and 10 in Eq. 7, gives:

$$\sum_{m=-\infty}^{+\infty}\sum_{n=-\infty}^{+\infty} \left[E_n A(k+g_m)(k+g_m+g_n) - \omega^2 \rho_n A\right] \tilde{u}_m e^{j(k+g_m+g_n)x} = 0. \tag{12}$$

Multiplying eq 12 by $e^{-j(k+g_r)x}/a$, with $g_r = 2\pi r/a$, and integrating from $-a/2$ to $a/2$, yields

$$\sum_{m=-\infty}^{+\infty}\sum_{n=-\infty}^{+\infty} \left[E_n A(k+g_m)(k+g_m+g_n) - \omega^2 \rho_n A\right] \tilde{u}_m \frac{1}{a}\int_{-a/2}^{a/2} e^{j(g_m+g_n-g_r)x} dx = 0. \tag{13}$$

Given that

$$\frac{1}{a}\int_{-a/2}^{a/2} e^{j(g_m+g_n-g_r)x} dx = \frac{1}{a}\int_{-a/2}^{a/2} e^{j2\pi/a(m+n-r)x} dx = \delta_{n,r-m} = \begin{cases} 1, & \text{if } n = r-m \\ 0, & \text{otherwise} \end{cases}, \tag{14}$$

where $\delta_{n,r-m}$ is the Kronecker delta. One can rewrite Eq. 13 as

$$\sum_{m=-\infty}^{+\infty} \left[E_{r-m} A(k+g_m)(k+g_r) - \omega^2 \rho_{r-m} A\right] \tilde{u}_m = 0. \tag{15}$$

Equivalently

$$\sum_{m=-\infty}^{+\infty} E_{r-m} A(k+g_m)(k+g_r)\tilde{u}_m = \lambda \sum_{m=-\infty}^{+\infty} \rho_{r-m} A \tilde{u}_m, \tag{16}$$

where $\lambda = \omega^2$. Equation 16 is a system with an infinite amount of equations. Thus, to solve this system, one can truncate the Fourier series to the first M terms, i.e., $r, m \in [-M, ..., M] \in \mathbb{Z}$, such that Eq. 16 can be rewritten as

$$\mathbf{B}\tilde{\mathbf{u}} = \lambda \mathbf{C}\tilde{\mathbf{u}}, \tag{17}$$

where the coefficients of vector $\tilde{\mathbf{u}}$ are $\tilde{u}_m$ and the coefficients of matrices $\mathbf{B}$ and $\mathbf{C}$ are given by:

$$B_{mr} = E_{r-m} A(k+g_m)(k+g_r),\ \ C_{mr} = \rho_{r-m} A. \tag{18}$$

Notice that Eq. 18 represents a generalized eigenvalue problem on $\lambda(k)$ and should be solved for each k, within FBZ or FIBZ.

4. NUMERICAL RESULTS

An infinite 1D PnC rod composed by two materials, aluminium and epoxy, is considered. This PnC is illustrated in Figure 1, where blue and white colours represent epoxy and aluminium, respectively. For the deterministic analysis, the length of aluminium part in the middle of unit cell is a_A = 0.05 m and the length of epoxy parts are a_B = 0.01 m, where subscripts A and B are associated with aluminium and epoxy, thus unit cell length $a = a_A + 2a_B$ = 0.07 m. PnC rod geometry and material properties are unit-cell length 0.07 m, width of 0.01m, height of 0.01, Young's modulus of aluminium of 77.6 GPa and epoxy as, 4.35 GPa, mass density of 2730 kg/m^3 and 1180 kg/m^3, respectively.

Figure 2 illustrates the band structure, real part of reduced Bloch wave vector versus frequency. By assuming $M = 10$ harmonic terms in Fourier series expansion, it implies that $m = \bar{m} = [-10, ..., 10]$, which means $2M + 1 = 21$ plane waves. The first bands and first Bragg-type band gaps are illustrated in Figure 2(b) by grey shaded regions. Whether the PnC rod is composed only by aluminium or by epoxy, i.e., a homogeneous rod, thus there is no Bragg scattering and band gaps are not opened up. In figure 2 it must be highlighted that the reduced Bloch wave vector does not have values higher than -1 and 1, since in PWE approach Bloch wave vector has only values within FBZ.

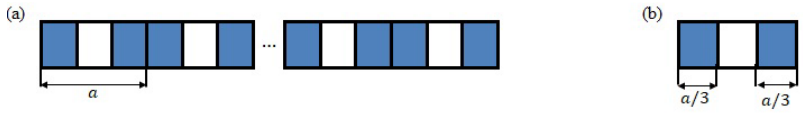

Figure 1. Schematic representation of the 1D PnC rod with unit cells of aluminium (white) and epoxy (blue) (a). PnC rod unit cell (b).

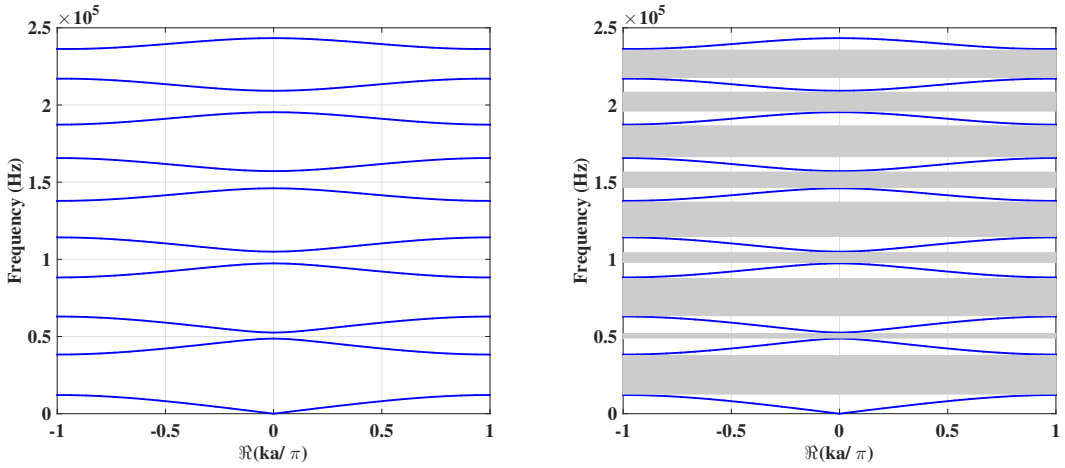

Figure 2. Band structure of the 1D PnC rod calculated by PWE approach, considering 21 plane waves (LHS). The first branches of the band structure and Bragg-type band gaps in grey shaded regions (RHS).

Next step includes the uncertainty in the Young's modulus and verifies the effect of randomness in the band gap. The first and second moments are used to demonstrate the variability in the band structure and Bragg-type band gaps. Geometrical and properties are the same of the deterministic case except for Young's modulus which in this case is assumed to be a random variable with a coefficient of variation of 10%, leads on the Lognormal distribution, as described in the previews section. The Lognormal distribution support is on the nonnegative axis and is widely used in practice to model random variables not allowed to have negative values. The first and second statical moments are calculated using the 300 samples obtained by the non-intrusive MC simulation.

Mean and the standard deviation envelope of the band structure of the 1D PnC rod calculated by PWE with 300 samples obtained by MC simulation is shown in figure 3. It can be noticed that the mean followed the deterministic result presented in fig 2(LHS). More variability in the response seems at the high-frequency range compared to the low-frequency, which is typical behaviour of dynamic systems. By comparing the deterministic and stochastic first branches of the band structure and Bragg-type band gaps in the grey shaded regions fig 2 and 3 (RHS), respectively, in the stochastic case significant part of the Bragg-type band gaps regions vanished due the variability associated.

Notably, the consideration of the random parameter causes some perturbation in the system. By considering the standard deviation envelop the band gap is more extensive in high frequencies that typical behaviour of dynamic system analysis. In general reducing the bandgap regions or the band gaps disappeared.

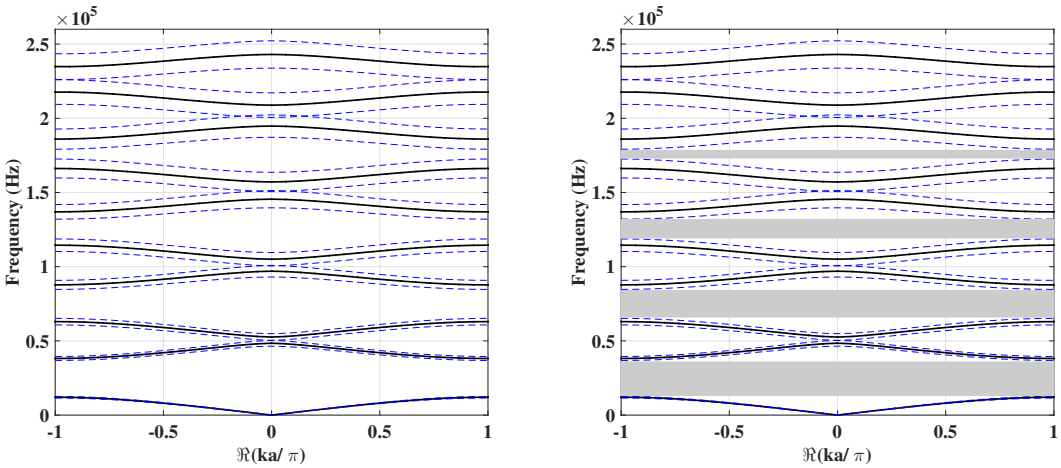

Figure 3. Mean (black continuous-line) and standard deviation envelope (blue dashed-line) of the band structure of the 1D PnC rod calculated by PWE approach, considering 21 plane waves (LHS). The first branches of the band structure and Bragg-type band gaps in grey shaded regions (RHS).

5. FINAL REMARKS

A study the influence of random properties established in Young's modulus can cause in the band structure of the 1D PnC, and in band gap regions was investigated . The uncertainty of the random variable kind was included in PWE the formulation for 1D phononic crystal rod. To generate samples for the statistical analysis, we used the nonintrusive MC Simulation. The stochastic model was validated by comparing the deterministic and with the first and second statistical moments of the band structure. The uncertainty associated in the model affects the band gap in a few frequency ranges, narrowing the band gaps width until completely vanishing.

6. REFERENCES

Doyle, J.F., 1997. *Wave propagation in structures : spectral analysis using fast discrete Fourier transforms*. Mechanical engineering. Springer-Verlag New York, Inc., New York, 2nd edition.

El-Naggar, S., 2012. "Dependency of the photonic band gaps in two-dimensional metallic photonic crystals on the shapes and orientations of rods." *Optical Engineering*, Vol. 51, No. 1, pp. 68001–68008.

Kushwaha, M., Halevi, P. and Martínez, G., 1994. "Theory of acoustic band structure of periodic elastic composites." *Physical Review B*, Vol. 49, No. 1, pp. 2313–2322.

Laude, V., Achaoui, Y., Benchabane, S. and Khelif, A., 2009. "Evanescent bloch waves and the complex band structure of phononic crystals." *Physical Review B*, Vol. 80(092301), No. 1, pp. 1–4.

Qian, Z.H., F.Jin, F.M.Li and Kishimoto, K., 2008. "Complete band gaps in two-dimensional piezoelectric phononic crystals with connectivity family". *International Journal of Solids and Structures*, Vol. 45, pp. 4748–4755.

Rubinstein, R.Y., 2008. *Simulation and the Monte Carlo Method, 2nd Edition*. Wiley.

Sampaio, R. and Lima, R., 2012. *Modelagem Estocástica e Geração de Amostras de Variáveis e Vetores Aleatórios*. SBMAC (Notas em Matemática Aplicada; v. 70).

Sigalas, M. and Economou, E., 1992. "Elastic and acoustic wave band structure." *Journal of Sound and Vibration*, Vol. 158, No. 1, pp. 377–382.

Sobol', I.M., 1994. *A primer for the Monte Carlo method*. CRC Press, New York, 1st edition.

Vasseur, J., Matar, O.B., Robillard, J., Hladky-Hennion, A. and Deymier, P., 2011. "Band structures tunability of bulk 2d phononic crystals made of magneto-elastic materials." *AIP Advances*, Vol. 1, pp. 41904–41915.

Wang, Y., Li, F., Huang, W., Jiang, X., Wang, Y. and Kishimoto, K., 2008. "Wave band gaps in two-dimensional piezoelectric/piezomagnetic phononic crystals." *International Journal of Solids and Structures*, Vol. 48, pp. 4203–4210.

Xiao, Y., Wen, J. and Wen, X., 2012a. "Broadband locally resonant beams containing multiple periodic arrays of attached resonators." *Physics Letters A*, Vol. 376(16), No. 1, pp. 1384–1390.

Xiao, Y., Wen, J. and Wen, X., 2012b. "Flexural wave band gaps in locally resonant thin plates with periodically attached spring-mass resonators." *Journal of Physics D: Applied Physics*, Vol. 45(19), No. 1, pp. 1–12.

Xiu, D., 2010. *Numerical Methods for Computations-A Spectral method approcah*. Princeton University Press, New Jersey, 1st edition.

7. RESPONSIBILITY NOTICE

The authors is are the only responsible for the printed material included in this paper.